M_{T2}-assisted on-shell reconstruction of missing momenta and its application to spin measurement at the LHC

Won Sang Cho, Kiwoon Choi, Yeong Gyun Kim and Chan Beom Park

Department of Physics, KAIST, Daejeon 305–017, Korea

Abstract

We propose a scheme to assign a 4-momentum to each WIMP in new physics event producing a pair of mother particles each of which decays to an invisible weakly interacting massive particle (WIMP) plus some visible particle(s). The transverse components are given by the value that determines the event variable M_{T2}, while the longitudinal component is determined by the on-shell condition on the mother particle. Although it does not give the true WIMP momentum in general, this M_{T2}-assisted on-shell reconstruction of missing momenta provides kinematic variables well correlated to the true WIMP momentum, and thus can be useful for an experimental determination of new particle properties. We apply this scheme to some processes to measure the mother particle spin, and find that spin determination is possible even without a good knowledge of the new particle masses.

PACS numbers:

The Large Hadron Collider (LHC) at CERN will explore soon the TeV energy scale where new physics beyond the Standard Model (SM) is likely to reveal itself. There are two major motivations for new physics at the TeV scale, one is the hierarchy problem and the other is the existence of dark matter (DM). Constraints from electroweak precision measurements and proton decay suggest that TeV scale new physics preserves a Z_2 parity under which the new particles are odd, while the SM particles are even. Well-known examples include the weak scale supersymmetry (SUSY) with conserved R-parity [1], little Higgs model with T-parity [2], and extra-dimensional model with KK-parity [3]. The lightest new particle in these models is typically a weakly interacting massive particle (WIMP) which is a good DM candidate.

A typical LHC signature of new physics model with conserved Z_2 parity is the production of a pair of new particles decaying to invisible WIMPs plus some visible SM particles. As the WIMP momenta can not be measured, an event by event reconstruction of the new particle's rest frame is not available, which makes the determination of new particle mass and spin quite non-trivial. For the mass measurement, several methods have been proposed so far [4, 5, 6], and they might work with certain accuracy depending upon the kinematic situation. One can also attempt to determine the spin from the production rate or from a kinematic variable distribution that shows spin correlation [7]. However, usually spin determination is more difficult as it requires a larger statistics and/or a good knowledge of the mass spectrum and branching ratios.

In this paper, we propose a scheme to assign a 4-momentum to each WIMP in new physics event, which can provide kinematic variables useful for the experimental determination of new particle properties, particularly the spin. We dub this scheme the "M_{T2}-Assisted On-Shell" (MAOS) reconstruction as the transverse components are given by the value that determines the collider variable M_{T2} [5], while the longitudinal component is determined by the on-shell condition imposed on the mother particle. This MAOS reconstruction of WIMP momenta can be done even without a good knowledge of the WIMP and mother particle masses. In the following, we discuss the MAOS reconstruction in more detail, and apply it to the 3-body decay of gluino and the 2-body decay of Drell-Yan produced slepton, as well as to their universal extra-dimension (UED) equivalents, in order to see the spin effects in these processes [8, 9].

To start with, let us consider the new physics process:

$$pp \to Y(1) + \bar{Y}(2) \to V(p_1)\chi(k_1) + V(p_2)\chi(k_2), \tag{1}$$

where $V(p)$ denotes generic set of visible SM particles with total 4-momentum p^μ and $\chi(k)$ is the WIMP with 4-momentum k^μ. For an event set of this type, one can introduce *trial* mother particle and WIMP masses, m_Y and m_χ, and impose the on-shell condition together with the missing E_T constraint:

$$(p_i + k_i)^2 = m_Y^2, \quad k_i^2 = m_\chi^2, \quad \mathbf{k}_{1T} + \mathbf{k}_{2T} = \mathbf{p}_T^{\rm miss}, \tag{2}$$

where $\mathbf{p}_T^{\rm miss}$ denotes the missing transverse momentum of the event. As these provide 6 constraints for 8 unknowns, k_i^μ $(i = 1, 2)$, there are 2-parameter family of solutions, which can be parameterized by $\mathbf{k}_{1T}$. For any choice of real $\mathbf{k}_{1T}$, e.g. $\mathbf{k}_{1T} = \tilde{\mathbf{k}}_T$, the longitudinal WIMP momenta are determined to be

$$k_{iL} = \frac{1}{(E_{iT}^V)^2}\left[p_{iL}A_i \pm \sqrt{p_{iL}^2 + (E_{iT}^V)^2}\sqrt{A_i^2 - (E_{iT}^V E_{iT}^\chi)^2}\right] \equiv \tilde{k}_{iL}^\pm, \tag{3}$$

where $E_{iT}^V = \sqrt{p_i^2 + |\mathbf{p}_{iT}|^2}$, $E_{iT}^\chi = \sqrt{m_\chi^2 + |\mathbf{k}_{iT}|^2}$, and $A_i = \frac{1}{2}(m_Y^2 - m_\chi^2 - p_i^2) + \mathbf{p}_{iT}\cdot\mathbf{k}_{iT}$ for $\mathbf{k}_{1T} = \tilde{\mathbf{k}}_T$ and $\mathbf{k}_{2T} = \mathbf{p}_T^{\rm miss} - \tilde{\mathbf{k}}_T$. It is obvious that $\tilde{k}_{iL}^\pm$ are real *if and only if* $|A_i| \geq E_{iT}^V E_{iT}^\chi$ which is equivalent to

$$m_Y \geq \max\{M_T^{(1)}, M_T^{(2)}\}, \tag{4}$$

where $M_T^{(i)} = \sqrt{p_i^2 + m_\chi^2 + 2(\, E_{iT}^V E_{iT}^\chi - \mathbf{p}_{iT}\cdot\mathbf{k}_{iT})}$ corresponds to the transverse mass of the mother particle $Y(i)$ with $\mathbf{k}_{1T} = \tilde{\mathbf{k}}_T$ and $\mathbf{k}_{2T} = \mathbf{p}_T^{\rm miss} - \tilde{\mathbf{k}}_T$.

In principle, one could choose event-by-event any value of $\tilde{\mathbf{k}}_T$. However, the condition (4) suggests that the *best* choice of $\tilde{\mathbf{k}}_T$ is the one minimizing $\max\{M_T^{(1)}, M_T^{(2)}\}$ for each event, i.e. the value giving the collider variable M_{T2} [5]:

$$M_{T2}(p_i, m_\chi) \equiv \min_{\mathbf{k}_{1T}+\mathbf{k}_{2T}=\mathbf{p}_T^{\rm miss}} \left[\max\{M_T^{(1)}, M_T^{(2)}\}\right], \tag{5}$$

where the minimization is performed over all possible WIMP transverse momenta $\mathbf{k}_{iT}$ under the constraint $\mathbf{k}_{1T} + \mathbf{k}_{2T} = \mathbf{p}_T^{\rm miss}$. For given trial masses $m_{\chi,Y}$, this choice of $\tilde{\mathbf{k}}_T$, which is unique for each event, allows the largest event set to have real $\tilde{k}_{iL}^\pm$. In the following, we call this scheme the M_{T2}-Assisted On-Shell (MAOS) reconstruction, which assigns one or both of the two 4-momenta

$$\tilde{k}^\pm = (\sqrt{m_\chi^2 + |\tilde{\mathbf{k}}_T|^2 + |\tilde{k}_L^\pm|^2}, \tilde{\mathbf{k}}_T, \tilde{k}_L^\pm), \tag{6}$$

to each WIMP in the new physics event (1)[1]. With these MAOS momenta, one can construct various kinematic variables whose distribution shape may provide information on new particle properties.

By construction, if $m_Y \geq M_{T2}^{\max}(m_\chi)$, where $M_{T2}^{\max}$ denotes the maximum of M_{T2} over the event set under consideration, the reconstructed MAOS momenta are real for all events. However, if $m_Y < M_{T2}^{\max}(m_\chi)$, generically there are some events which do not allow real longitudinal MAOS momenta. Also by construction, for the M_{T2} end-point events with $M_{T2} = M_{T2}^{\max}$, the MAOS momentum is same as the true WIMP momentum if (i) the trial masses used for reconstruction are same as the true masses, and (ii) the considered event set is large enough to give $M_{T2}^{\max}(m_\chi = m_\chi^{\rm true}) = m_Y^{\rm true}$. (Note that $M_{T2}^{\max}(m_\chi = m_\chi^{\rm true}) \leq m_Y^{\rm true}$ for generic event (sub)set, and the bound is saturated if the full event set is taken into account.) One can also find that $\tilde{k}_L^+ = \tilde{k}_L^-$ for an event whose M_{T2}-value is same as m_Y, which obviously includes the end-point event when the trial mother particle mass is chosen as $m_Y = M_{T2}^{\max}(m_\chi)$. In fact, the most interesting feature of the MAOS momenta, which will be discussed below with a specific example, is that they are distributed around the true WIMP momentum with non-trivial correlation even when constructed with generic trial WIMP and mother particle masses.

As a specific application of the MAOS reconstruction, we first consider the symmetric 3-body decays of gluino pair in SUSY model, $\tilde{g} + \tilde{g} \to q\bar{q}\chi + q\bar{q}\chi$, and also the similar decays of KK gluon pair in UED-like model. For SUSY case, we choose the focus (SPS2) point of mSUGRA scenario which gives the following weak scale masses: $m_{\tilde{g}}^{\rm true} = 779$ GeV, $m_\chi^{\rm true} = 122$ GeV, and $m_{\tilde{q}}^{\rm true} \simeq 1.5$ TeV. We also consider its UED equivalent in which the gluino is replaced with the first KK gluon $g_{(1)}$, the Bino $\tilde{B}$ with the first KK $U(1)_Y$ boson $B_{(1)}$, and squarks with the first KK quarks. Using `MadGraph/MadEvent` [10], we have generated the events at parton-level for both SUSY and UED cases, and constructed the MAOS momentum $\tilde{k}^\pm$. We then examined the distribution of $\Delta\tilde{k} \equiv \tilde{k}^\pm - k^{\rm true}$ for both SUSY and UED event sets with various choices of trial masses $m_{\chi,Y}$ and also of the event subset selected by their M_{T2} values. We found that the distribution of $\Delta\tilde{k}_T$ is always peaked at zero for generic value of m_χ, and its width gets narrower if one considers an event subset including

[1] For simplicity, here we consider the production of $Y\bar{Y}$ in which the up-streaming momentum is negligible. It is however straightforward to generalize the MAOS reconstruction to the process with a sizable up-streaming momentum.

only the near end-point events of M_{T2}. On the other hand, the distribution of $\Delta\tilde{k}_L$ is more chaotic, partly because of the error propagation from $\Delta\tilde{k}_T$ and also the two-fold degeneracy of the longitudinal component. Still it is peaked at zero, although the width is significantly broader, for a wide range of (m_χ, m_Y) which includes the case with $m_Y = M_{T2}^{\max}(m_\chi)$. As an example, we depict in Fig. 1 the distributions of $\Delta\tilde{k}_{T,L}$ (including both of $\tilde{k}_L^\pm$) for the MAOS momenta of the SPS2 SUSY event set, which has been constructed with $m_\chi = 0$ and $m_Y = M_{T2}^{\max}(m_\chi = 0)$. Fig. 1a shows the distributions of the full event set, while Fig. 1b is for a subset including only the top 10% end-point events of M_{T2}. We can see that the MAOS momentum has a good correlation with the true momentum even for the full event set, and the correlation becomes stronger for the near end-point events of M_{T2}. This suggests that if one has an enough statistics, it can be more efficient to do MAOS reconstruction using only the near end-point events.

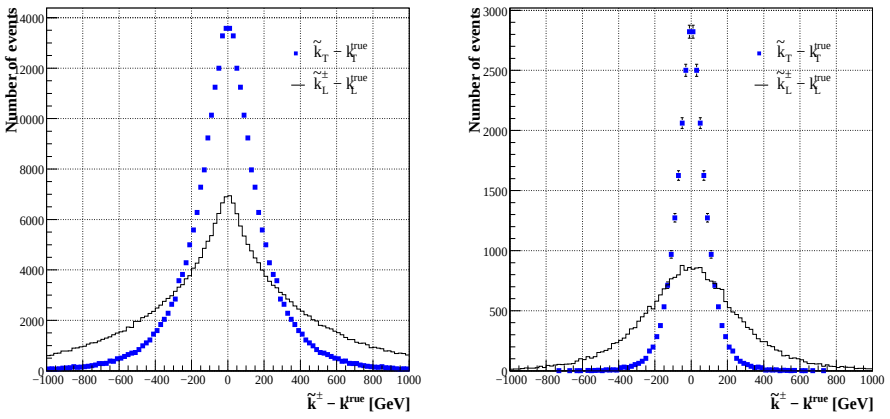

FIG. 1: The distributions of $\tilde{k}^\pm - k^{\rm true}$ for (a) the full event set, and (b) the top 10% end-point events of M_{T2}. Here the MAOS momenta were constructed with $m_\chi = 0$ and $m_Y = M_{T2}^{\max}(m_\chi = 0)$.

If one could measure all final state momenta in the 3-body decay,

$$Y \to q(p_q)\bar{q}(p_{\bar{q}})\chi(k), \tag{7}$$

where $Y = \tilde{g}$ or $g_{(1)}$, and $\chi = \tilde{B}$ or $B_{(1)}$, the spin of Y can be determined by the 2-D invariant mass distribution $dN_{\rm decay}/dm_{qq}^2 dm_{q\chi}^2$ for $m_{qq}^2 = (p_q + p_{\bar{q}})^2$ and $m_{q\chi}^2 = (p_q + k^{\rm true})^2$ or $(p_{\bar{q}} + k^{\rm true})^2$. However, as the true WIMP momentum is not available, one could have only the m_{qq}^2-distribution, $dN_{\rm decay}/dm_{qq}^2 = \int dm_{q\chi}^2 dN_{\rm decay}/dm_{qq}^2 dm_{q\chi}^2$. In [8], it was found

that the SUSY and UED m_{qq}^2-distributions show a difference in small m_{qq}^2 limit, however this difference might be difficult to be seen in the real data unless the mass ratio $m_Y^{\rm true}/m_\chi^{\rm true}$ is quite large, e.g. bigger than 7 or 8.

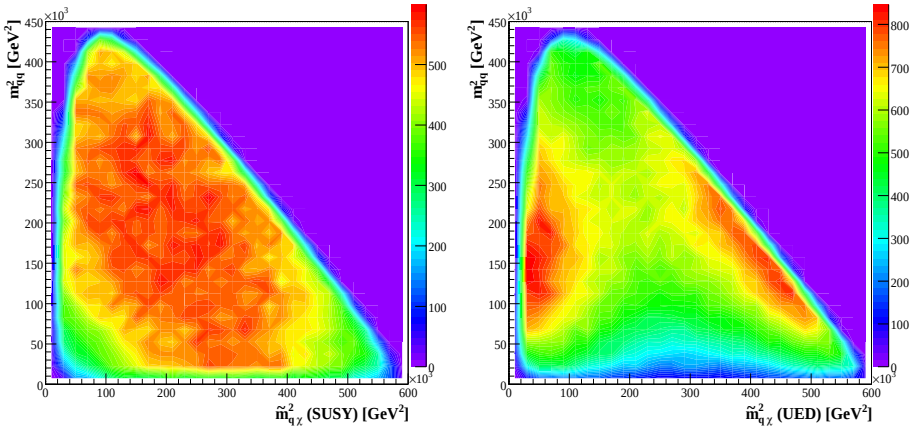

FIG. 2: SUSY and UED Dalitz plots of m_{qq}^2 and $\tilde{m}_{q\chi}^2$ at parton level for $m_{\chi,Y} = m_{\chi,Y}^{\rm true}$ and very large luminosity.

On the other hand, with the MAOS momenta $\tilde{k}^\pm$, we can do a much better job as the event distribution $dN_{\rm event}/dm_{qq}^2 d\tilde{m}_{q\chi}^2$ is available, where

$$\tilde{m}_{q\chi}^2 = (p_q + \tilde{k}^\pm)^2 \quad \text{or} \quad (p_{\bar{q}} + \tilde{k}^\pm)^2. \tag{8}$$

In Fig. 2, we depict this MAOS distribution including both $\tilde{k}^+$ and $\tilde{k}^-$ for the SUSY SPS2 point with $m_{\chi,Y} = m_{\chi,Y}^{\rm true}$ and its UED equivalent in the ideal limit of no combinatorial error and very large luminosity[2]. The results show a clear difference, with which one can distinguish SUSY and UED unambiguously. In fact, these MAOS distributions reproduce excellently the shape of the true invariant mass distributions $dN_{\rm decay}/dm_{qq}^2 dm_{q\chi}^2$ constructed with the true WIMP momentum $k^{\rm true}$ [11].

To see the feasibility of the MAOS reconstruction in realistic situation, we analyzed the event sets of the same SUSY and UED points, but now with the integrated luminosity $\mathcal{L} = 300\,{\rm fb}^{-1}$. To suppress the backgrounds, we employed an appropriate selection cut commonly taken for new physics events at the LHC, and adopted the hemisphere method

[2] In fact, one can use only $\tilde{k}^+$ or only $\tilde{k}^-$ for the MAOS invariant mass distribution, and still finds the same shape of distribution.

to deal with the combinatorial problem. We also included the smearing effects on the momentum resolution. The results for $m_{\chi,Y} = m_{\chi,Y}^{\rm true}$ are depicted in Fig. 3, which still shows a clear difference between SUSY and UED.

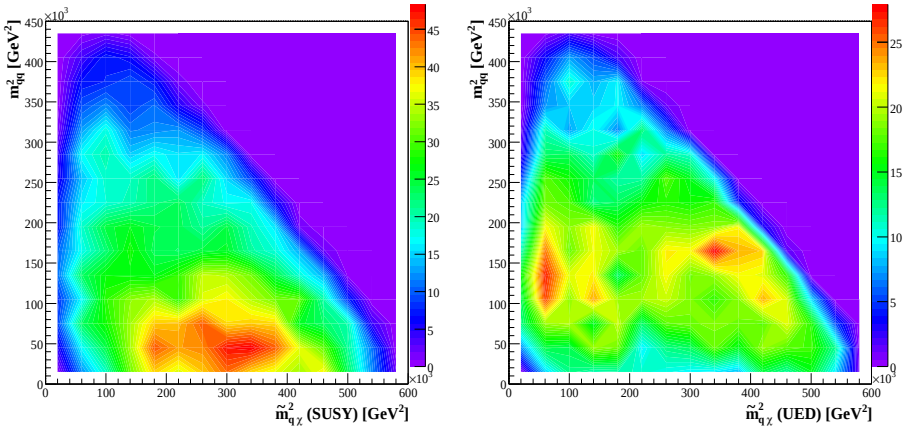

FIG. 3: SUSY and UED Dalitz plots of m_{qq}^2 and $\tilde{m}_{q\chi}^2$ for $m_{\chi,Y} = m_{\chi,Y}^{\rm true}$ and $\mathcal{L} = 300\,{\rm fb}^{-1}$, including the combinatorial error and smearing effects under a proper event cut.

A nice feature of the MAOS reconstruction is that it does not require any pre-knowledge of the mother particle and WIMP masses. To see if the spin measurement is possible without a good knowledge of new particle masses, we have repeated the analysis for a wide range of $m_{\chi,Y}$. We then found that the basic feature of distribution is retained even when the trial masses used for the reconstruction are very different from the true masses, and SUSY and UED can be clearly distinguished in all cases [11]. We depict the result for one example in Fig. 4, which is for the case of $m_\chi = 0$ and $m_Y = M_{T2}^{\rm max}(m_\chi = 0)$, and the result includes the combinatorial error and detector smearing effects under a proper event cut.

Once the MAOS WIMP momenta are available, the MAOS momenta of mother particles can be reconstructed also. One can then investigate the production angular distribution of mother particle pair in their center of mass frame, which may provide information on the spin of mother particle. As an example, we have considered the Drell-Yan pair production of Y (= the slepton $\tilde{l}$ or the KK lepton $l_{(1)}$) [9],

$$q\bar{q} \to Z^0/\gamma \to Y + \bar{Y} \to l^+(p_1)\chi(k_1) + l^-(p_2)\chi(k_2), \tag{9}$$

and generated the events for the SPS1a SUSY point ($m_{\tilde{l}_R}^{\rm true} = 143$ GeV, $m_\chi^{\rm true} = 96$ GeV) and its UED equivalent.

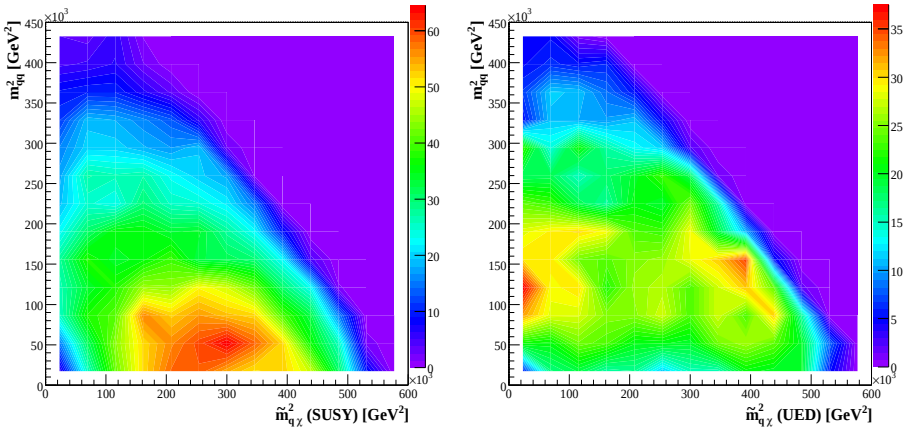

FIG. 4: SUSY and UED Dalitz plots of m^2_{qq} and $\tilde{m}^2_{q\chi}$ for $m_\chi = 0$, $m_Y = M_{T2}^{\max}(m_\chi = 0)$ and $\mathcal{L} = 300\,\mathrm{fb}^{-1}$, including the combinatorial error and smearing effects under a proper event cut.

As slepton is a scalar particle, the angular distribution is proportional to $1-\cos^2\theta^*$, where θ^* is the production angle with respect to the proton beam direction. On the other hand, the corresponding Drell-Yan production of KK leptons shows the characteristic distribution of spin-half particles, which is proportional to $1+\cos^2\theta^*(E^2_{l_1}-m^2_{l_1})/(E^2_{l_1}+m^2_{l_1})$ [9]. One may then examine the lepton angular distribution in the center of rapidity frame of $l\bar{l}$, which would reflect the qualitative feature of the above θ^*-dependence of the mother particle distribution [9].

Again, we can do a much better job with the MAOS momenta $\tilde{k}^\pm_i$ $(i = 1, 2)$ as we can probe the angular distribution of the mother particle MAOS momenta. To see this, we have reconstructed the MAOS momenta, $p_i + \tilde{k}^\pm_i$, of the slepton pair and of the KK lepton pair, and examined their angular distribution in the center of mass frame while including the four different combinations of MAOS momenta, i.e. $(\tilde{k}^\alpha_1, \tilde{k}^\beta_2)$ with $\alpha, \beta = \pm$, altogether. Since it depends on the longitudinal boost to the center of mass frame, the shape of angular distribution is somewhat sensitive to the trial mother particle and WIMP masses. To minimize this sensitivity, we have chosen $m_Y = M_{T2}^{\max}(m_\chi)$ and imposed the event selection cut including only the top 10% of the events near the end-point of M_{T2}. We also included the detector smearing effect on the lepton momentum resolution. In Fig. 5a, we depict the resulting SUSY and UED angular distributions for $m_{\chi,Y} = m^{\mathrm{true}}_{\chi,Y}$ and $\mathcal{L} = 300\,\mathrm{fb}^{-1}$, and compare them to the angular distributions obtained from the true WIMP

momenta. The result shows that the MAOS angular distribution excellently reproduces the true production angular distribution, with which one can clearly distinguish SUSY from UED.

To see how much the distribution shape is sensitive to the trial masses, we repeat the analysis, but now with $m_\chi = 0$ and $m_Y = M_{T2}^{\max}(m_\chi = 0)$. The result depicted in Fig. 5b shows that the distribution has basically the same shape as the case (Fig. 5a) with $m_{\chi,Y} = m_{\chi,Y}^{\rm true}$.

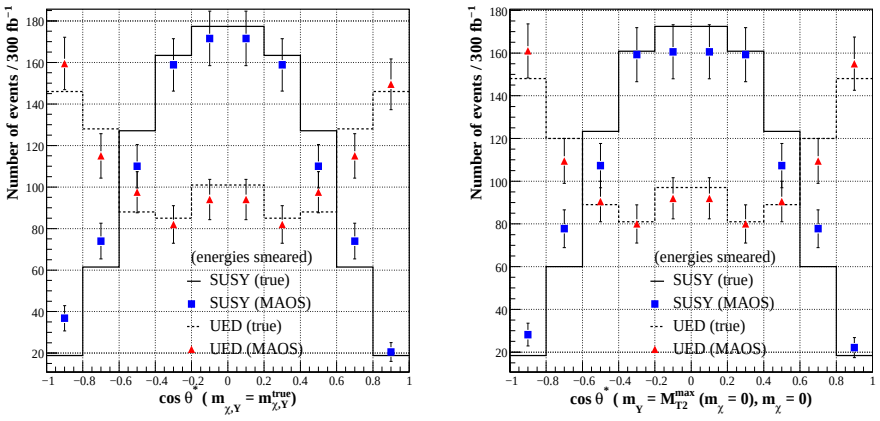

FIG. 5: Slepton and KK-lepton production angular distributions constructed with the true momenta and the MAOS momenta for $\mathcal{L} = 300\,\mathrm{fb}^{-1}$: (a) $m_{\chi,Y} = m_{\chi,Y}^{\rm true}$ and (b) $m_\chi = 0$, $m_Y = M_{T2}^{\max}(m_\chi = 0)$.

To conclude, we have proposed a scheme, the M_{T2}-assisted on-shell (MAOS) reconstruction, to assign 4-momenta to the WIMP pair in generic new physics event of the type (1). Introducing a trial WIMP mass which is common to the whole event set under consideration, the transverse MAOS momenta of each event are determined by the transverse momentum that gives the event variable M_{T2}. On the other hand, the longitudinal MAOS momenta are determined by the on-shell condition defined with a trial mother particle mass which is again common to the whole event set. With these MAOS WIMP momenta, one can construct various kinematic variable distributions which would not be available before, and extract information on new particle properties from those distributions. In this paper, we considered an application of the MAOS reconstruction to the 3-body decays of the pair-produced gluinos and also to the 2-body decays of the Drell-Yan produced charged slepton

pair to discriminate them from their UED equivalents. Our analysis suggests that the MAOS reconstruction of WIMP momenta provides a powerful tool for spin measurement, which can be viable even when a good knowledge of the new particle masses is not available. In the forthcoming paper [11], we will provide a more extensive discussion of the MAOS reconstruction and its applications, including some other processes to measure the new particle properties.

Acknowledgments

This work was supported by the KRF Grants funded by the Korean Government (KRF-2005-210-C0006 and KRF-2007-341-C00010), and the BK21 program of Ministry of Education.

---

[1] H. P. Nilles, *Phys. Rept.* **110** (1984) 1; H. E. Haber and G. L. Kane, *Phys. Rept.* **117** (1985) 75.

[2] N. Arkani-Hamed, A. G. Cohen and H. Georgi, *Phys. Lett.* **B513** (2001) 232 [hep-ph/0105239]; H. C. Cheng and I. Low, *JHEP* **0309** (2003) 051 [hep-ph/0308199].

[3] T. Appelquist, H. C. Cheng and B. A. Dobrescu, *Phys. Rev.* **D64** (2001) 035002 [hep-ph/0012100].

[4] I. Hinchliffe, F. E. Paige, M. D. Shapiro, J. Soderqvist and W. Yao, *Phys. Rev.* **D55** (1997) 5520 [hep-ph/9610544]; H. Bachacou, I. Hinchliffe and F. E. Paige, *Phys. Rev.* **D62** (2000) 015009 [hep-ph/9907518]; B. C. Allanach, C. G. Lester, M. A. Parker and B. R. Webber, *JHEP* **0009** (2000) 004 [hep-ph/0007009]; K. Kawagoe, M. M. Nojiri and G. Polessello, *Phys. Rev.* **D71** (2005) 035008 [hep-ph/0410160]; H. C. Cheng, D. Engelhardt, J. F. Gunion, Z. Han and B. McElrath, *Phys. Rev. Lett.* **100** (2008) 252001 [arXiv:0802.4290].

[5] C. G. Lester and D. J. Summers, *Phys. Lett.* **B463** (1999) 99 [hep-ph/9906349]; A. J. Barr, C. G. Lester and P. Stephens, *J. Phys.* **G29** (2003) 2343 [hep-ph/0304226].

[6] W. S. Cho, K. Choi, Y. G. Kim and C. B. Park, *Phys. Rev. Lett.* **100** (2008) 171801 [arXiv:0709.0288]; B. Gripaios, JHEP **0802**, 053 (2008) [arXiv:0709.2740]; A. J. Barr, B. Gripaios and C. G. Lester, *JHEP* **0802** (2008) 014 [arXiv:0711.4008]; W. S. Cho, K.

Choi, Y. G. Kim and C. B. Park, *JHEP* **0802** (2008) 035 [arXiv:0711.4526].

[7] A. J. Barr, *Phys. Lett.* **B596** (2004) 205 [hep-ph/0405052]; J. M. Smillie and B. R. Webber, *JHEP* **0510** (2005) 069 [hep-ph/0507170]; A. K. Datta, G. L. Kane and M. Toharia, hep-ph/0510204; A. K. Datta, K. Kong and K. T. Matchev, *Phys. Rev.* **D72** (2005) 096006 [hep-ph/0509246]; L. T. Wang and I. Yavin, *JHEP* **0704** (2007) 032 [hep-ph/0605296]; G. L. Kane, A. A. Petrov, J. Saho and L. T. Wang, arXiv:0805.1397; M. Burns, K. Kong, K. T. Matchev, M. Park, arXiv:0808.2472.

[8] C. Csaki, J. Heinonen and M. Perelstein, *JHEP* **0710** (2007) 107 [arXiv:0707.0014].

[9] A. J. Barr, *JHEP* **0602** (2006) 042 [hep-ph/0511115].

[10] J. Alwall, P. Demin, S. Visscher, R. Frederix, M. Herquet, F. Maltoni, T. Plehn, D. L. Rainwater and T. Stelzer, *JHEP* **0709** (2007) 028 [arXiv:0706.2334].

[11] W. S. Cho, K. Choi, Y. G. Kim and C. B. Park, in preparation.